



Luminescence Hot Paper

Multistage Stimulus-Responsive Room Temperature Phosphorescence Based on Host–Guest Doping Systems

Yu Tian, Jie Yang, Zhenjiang Liu, Mingxue Gao, Xiaoning Li, Weilong Che, Manman Fang,* and Zhen Li*

Abstract: Compared with inorganic long-lasting luminescent materials, organic room temperature phosphorescent (RTP) ones show several advantages, such as flexibility, transparency, solubility and color adjustability. However, organic RTP materials close to commercialization are still to be developed. In this work, we developed a new host–guest doping system with stimulus-responsive RTP characteristics, in which triphenylphosphine oxide (**OPph₃**) acted host and benzo-(dibenzo)phenothiazine dioxide derivatives as guests. Turn-on RTP effect was realized by mixing them together through co-crystallization or grinding, in which the efficient energy transfer from host to guest and the strong intersystem crossing (ISC) ability of the guest have played significant role. Further on, multistage stimulus-responsive RTP characteristics from grinding to chemical stimulus were achieved via introducing pyridine group into the guest molecule. In addition, the anti-counterfeiting printings were realized for these materials through various methods, including stylus printing, thermal printing and inkjet printing, which brings RTP materials closer to commercialization.

Organic RTP materials, also known as organic afterglow materials, are organic systems with triplet emission at room temperature developed in recent years.^[1] Because phosphorescence has the characteristics of large Stokes shift, long lifetime and full utilization of excited state energy, it has received extensive attention from scientists and industry in the fields of organic optoelectronic materials,^[2] biological imaging,^[3] and anti-counterfeiting labels.^[4]

In recent years, the preparation and application of pure organic RTP materials have made great progress, especially the single-component system.^[5] Though accessing to and from the triplet state is a forbidden process for organic luminogens

and once thought to be too inefficient to be realized at room temperature, recent advances have vastly increased ISC efficiency by enhancing spin-orbit coupling (SOC) with the use of heteroatoms,^[6] heavy atoms,^[7] and multimers.^[8] However, most of them rely on special crystal structures^[9] with certain maintaining difficulties in cultivation and practical applications, which greatly limits actual application scenarios. In addition, some multi-component phosphorescent systems have been developed, mainly through co-crystallization, rigid matrix encapsulation, hardening in the polymer matrix, or interacting with other molecules of the same or different types.^[10] However, in actual operation, the preparation process of these multi-component materials is slightly complicated, and the application conditions are also subject to certain restrictions, especially in terms of flexibility. Based on this, RTP materials based on host–guest doping systems that do not rely on crystalline are most likely to solve the above problems. Although this kind of materials has been reported sporadically, the systematic studies are still scarce.^[11] Therefore, the mechanism and influencing factors of their RTP generation need to be further studied in detail, because this is important for the design of efficient RTP materials.

Compared with commonly phosphorescent materials, RTP materials with stimulus response effect, especially those that don't rely on special crystal forms, have advantages and commercial value in application fields such as anti-counterfeiting, sensing, and detection.^[9b,11b,12] Herein, we construct a series of guest molecules (energy acceptors), namely **Pph**, **BPph** and **DBPph** (Figure 1 b), which can be mixed with the host **OPph₃** (energy donor) to realize turn-on RTP effect by co-crystallization or grinding for the promotion of energy transfer between them (Figure 1 a). Among them, **BPph** doped system exhibits the best RTP performance, in which efficient energy transfer from host to guest and the strong ISC ability of the guest molecules are found to play the significant role (Figures 1 c and d). In addition, the introduction of pyridine group into guest molecules endows the resultant doping system with acid-base reversible and acid-heat reversible stimulus-responsive RTP effects. With this, the multistage stimulus-responsive RTP characteristic from grinding to chemical stimulus is achieved for the first time.

The photophysical properties related to **Pph**, **BPph**, **DBPph** and **OPph₃** in tetrahydrofuran solution (10^{-5} M) at room temperature were measured, as well as their solid powders (Figure S2 and Table S2). The UV-vis absorption spectra show that the maximum absorption wavelengths of them are 370 nm, 361 nm, 330 nm and 221 nm (Figure S2a), respectively, which accord with their conjugation degrees. Single components of **BPph**, **DBPph** and **OPph₃** show no

[*] Y. Tian, J. Yang, Z. Liu, M. Gao, X. Li, W. Che, Dr. M. Fang, Prof. Z. Li
Institute of Molecular Aggregation Science, Tianjin University
Tianjin 300072 (China)
E-mail: manmanfang@tju.edu.cn
lizhentju@tju.edu.cn

Prof. Z. Li
Department of Chemistry, Wuhan University
Wuhan 430072 (China)
and
Joint School of National University of Singapore and Tianjin
University, International Campus of Tianjin University
Binhai New City, Fuzhou 350207 (China)
E-mail: lizhen@whu.edu.cn

Supporting information and the ORCID identification number(s) for the author(s) of this article can be found under:
<https://doi.org/10.1002/anie.202107639>.

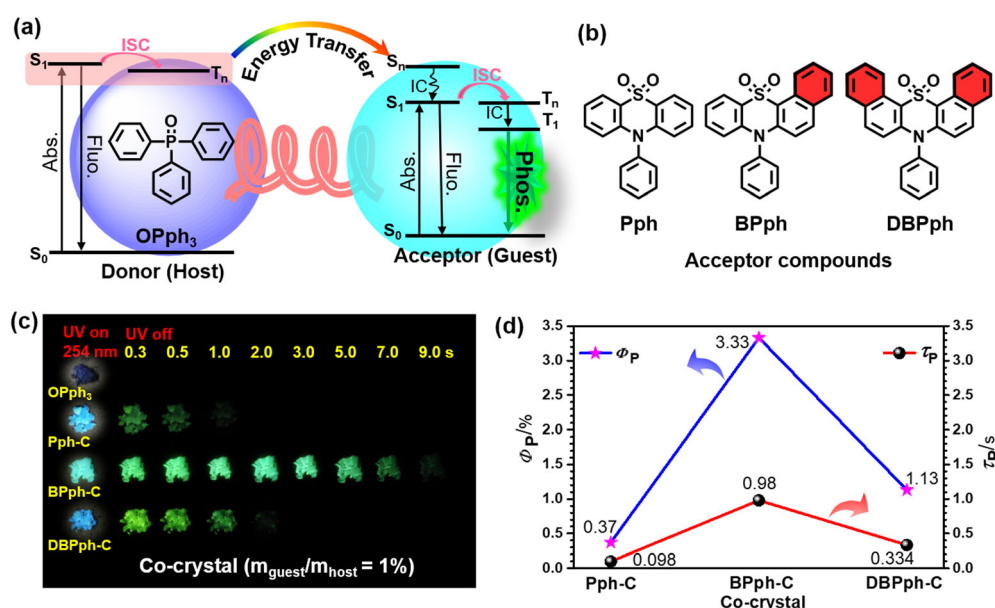


Figure 1. a) Energy transfer between donor (host) and acceptor (guest). b) Molecular structures of acceptors in this work. c) Photographs of co-crystals under and after excitation, $\lambda_{\text{ex}} = 254$ nm, $m_{\text{guest}}/m_{\text{host}} = 1\%$. “Pph-C” represents the co-crystal formed by mixing Pph and OPph_3 . d) Phosphorescence quantum yields and lifetimes of Pph-C, BPph-C and DBPph-C.

RTP phenomena (Figure S3 and Table S2), while a strong afterglow with a duration of ≈ 9 s is observed from a co-crystal sample of BPph-C ($\Phi_p = 3.33\%$, $\tau_p = 980$ ms) obtained by removing the solvent from a solution of BPph and OPph_3 (1:100, mass ratio) in ethanol. On the other hand, only weak RTP can be observed from co-crystals of Pph-C ($\Phi_p = 0.37\%$, $\tau_p = 98$ ms) and DBPph-C ($\Phi_p = 1.13\%$, $\tau_p = 334$ ms) (Figure 1c,d and S4c). The PL spectrum of BPph-C shows emission bands at 295 nm and 399 nm, which are attributed to the characteristic emission peaks of OPph_3 and BPph, respectively, and the new emission band ranging from 460–620 nm is considered to be the spectrum of the green afterglow (Figure S4a and S4b).

The phosphorescence spectrum (Figure S8b) of BPph in tetrahydrofuran solution (10^{-5} M) at 77 K is consistent with the RTP spectrum (Figure S4b) of BPph-C, which indicates the green afterglow of BPph-C is derived from the triplet emission of BPph. DBPph-C exhibits similar properties to BPph-C with its phosphorescence emission at 519 nm, while Pph-C gives two distinct emission bands, at 390–440 nm and 460–620 nm, respectively (Figure S4b). Compared to the low temperature phosphorescence spectrum (Figure S8a) of Pph solution, the RTP emission band at 460–620 nm is considered to be caused by the dimer in Pph aggregates, which may be caused by the non-uniform dispersion of guest molecules in the host.

Now two problems must be solved urgently. One is why RTP can be achieved from co-crystals, and the other is why the phosphorescence efficiencies and lifetimes of these three co-crystals are so different.

To answer these two questions, the emission spectrum of the host and the absorption spectra of the guests were compared. As shown in Figure 2a, the emission band of

OPph_3 crystal is at 295 nm, which shows large overlap with the absorption of guest molecules. So, it is considered that their energy levels are matched to a certain extent. In addition, the emission lifetime of OPph_3 crystal at 295 nm is 8.64 ns, while in co-crystal systems of Pph-C, BPph-C, and DBPph-C, the emission lifetimes at 295 nm are shortened to 6.63 ns, 4.95 ns and 6.01 ns (Figure 2b), respectively. This means the energy transfer from host to guest, and the corresponding efficiencies are calculated to be 23%, 43% and 30% (Figure 2c), respectively. It can be seen from Figure 2a, the absorption capacity of Pph under same concentration is the

worst, which is considered to be one of the reasons for its lowest energy transfer efficiency. On the other hand, DBPph and BPph give similar absorption ability to the emission from host. Further on, the energy levels of singlet and triplet excited states were calculated by TD-DFT based on their single crystal structures (Table S4 to S7). The energy of the S_1 state for OPph_3 is 5.60 eV (Table S4), and the S_n states of guests with energy within $E_{S_1} \pm 0.3$ eV of OPph_3 were enumerated (Figure S9 to S11), in which the energy transfer from OPph_3 to guest could occur easily. As shown in Figure S10, BPph-C has four energy levels (5.31 eV, 5.70 eV, 5.77 eV and 5.85 eV, respectively) that can be matched with the S_1 state of OPph_3 to realize energy transfer, while Pph-C and DBPph-C have only two (5.55 eV and 5.79 eV, Figure S9) and three (5.35 eV, 5.50 eV and 5.65 eV, Figure S11) matched energy levels, respectively. These results may further explain why the most effective energy transfer occurs in co-crystal system of BPph-C.

After energy transfer, the triplet emission ability of guest should be another important factor to affect the resultant RTP emission of co-crystal. In order to explain these phenomena in more depth, spin-orbit coupling constants (ξ) between S_1 and T_n for OPph_3 , Pph-C, BPph-C, and DBPph-C were analyzed in detail and the energy levels considered suitable for ISC were listed (Figures 2d, e, f and S12). As shown in Figure S12, although in OPph_3 , there are larger coupling constants between S_1 and T_{11}/T_{13} , which are 1.28 cm^{-1} and 3.50 cm^{-1} respectively, the coupling constant between T_1 and S_0 is only 0.24 cm^{-1} , indicating the weak phosphorescence emission ability from T_1 to S_0 . This is considered to be the reason why OPph_3 itself does not produce RTP. Pph, BPph, and DBPph all have good ISC ability from T_1 to S_0 (Figures 2d, e and f), and their coupling

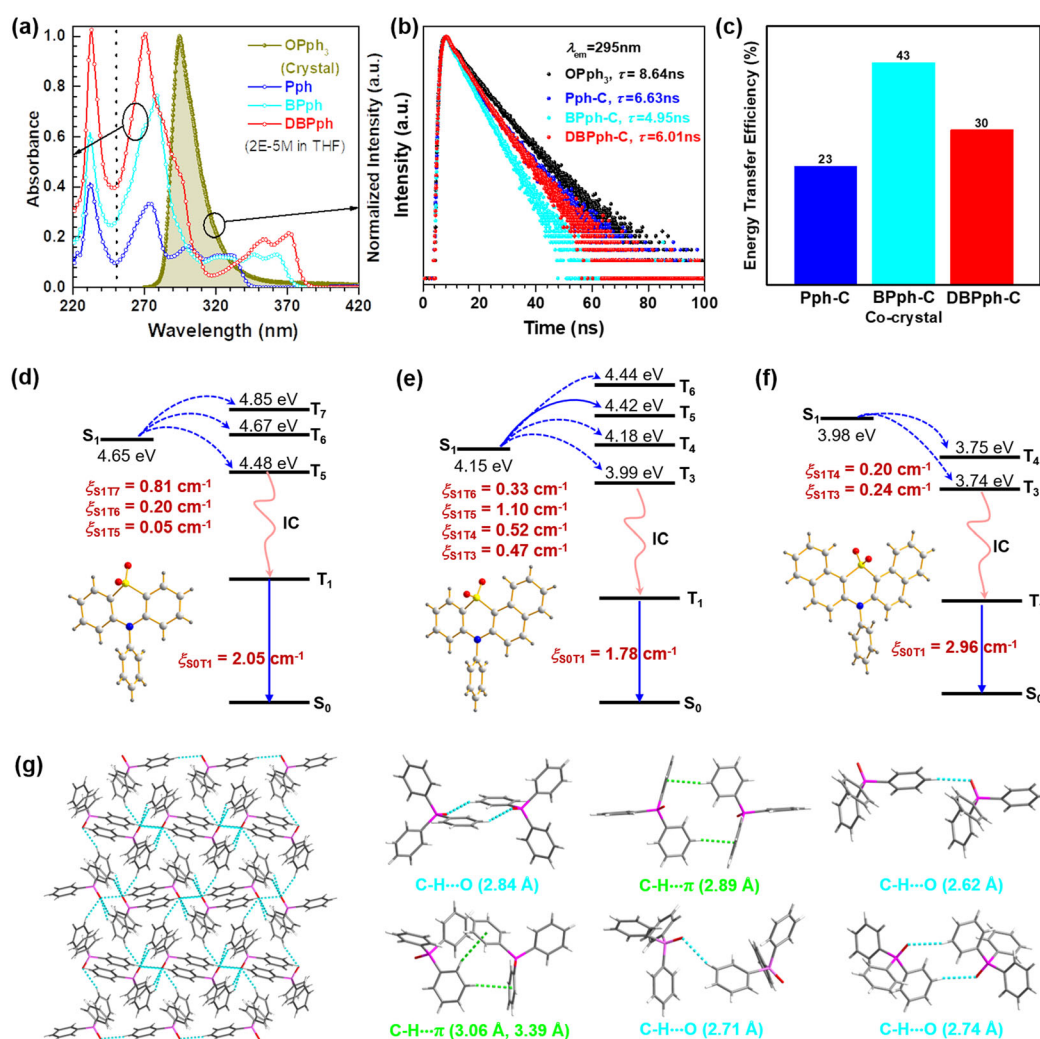


Figure 2. a) The PL spectrum of **OPph₃** crystal and the UV-vis absorption spectra of **Pph**, **BPph** and **DBPph** in tetrahydrofuran solution. b) Emission decay characteristics ($\lambda_{em} = 295$ nm) of **OPph₃** crystal and three co-crystals. c) Energy transfer efficiencies of **OPph₃** in three co-crystals. Theoretically-calculated energy levels and spin-orbit coupling constants (ξ) between S_1 and T_n based on the corresponding molecular geometries of **Ppy** (d), **Bppy** (e) and **DBppy** (f). Solid blue arrows represent major ISC channels with ξ over 1 cm^{-1} , and dashed blue arrows represent minor ISC channels with ξ less than 1 cm^{-1} . The black solid triplet states are those levels with energy within $E_{S_{1\pm}} \pm 0.3\text{ eV}$. g) Molecular packing (left) and intermolecular interactions (right) of **OPph₃**.

constants are 2.05 cm^{-1} , 1.78 cm^{-1} and 2.96 cm^{-1} , respectively. However, compared with **Pph** ($\xi_{S_{1T7}} = 0.81\text{ cm}^{-1}$, $\xi_{S_{1T6}} = 0.20\text{ cm}^{-1}$, $\xi_{S_{1T5}} = 0.05\text{ cm}^{-1}$) and **DBPph** ($\xi_{S_{1T4}} = 0.20\text{ cm}^{-1}$, $\xi_{S_{1T3}} = 0.24\text{ cm}^{-1}$), there are more T_n states that match S_1 with larger coupling constant in **BPph**, which are 0.33 cm^{-1} ($\xi_{S_{1T6}}$), 1.10 cm^{-1} ($\xi_{S_{1T5}}$), 0.52 cm^{-1} ($\xi_{S_{1T4}}$) and 0.47 cm^{-1} ($\xi_{S_{1T3}}$), respectively. So, the ISC ability of guest itself is also believed to have a certain impact on the phosphorescence efficiency and lifetime. Lastly, the good crystallinity of the host provides a suitable rigid environment for the guest, which can inhibit the non-radiative transition of the guest. Figure 2g shows **OPph₃** can be tightly packed by a large amount of C–H \cdots O ($2.62\text{--}2.84\text{ \AA}$) and C–H \cdots π ($2.89\text{--}3.39\text{ \AA}$) intermolecular interactions, which is beneficial to restrict thermal motion of molecule and oxygen diffusion, then contributing much to the resultant RTP emission in co-crystals.

Not only in co-crystal, obvious RTP emission could also be observed for the mixtures of host and guest samples after

grinding (Figure S13–S21 and Table S8), as long as the host and the guest are in contact with each other at an appropriate distance to occur energy transfer. As illustrated in Figure S19, a gradually enhanced and prolonged RTP emission could be realized with the increase of grinding time for a mixture of **BPph** and **OPph₃** (1:100 for mass ratio, namely **BPph-G**). At about 20 min, a greenish afterglow lasting ≈ 3 seconds was observed under ambient conditions. During the grinding process, the energy transfer efficiency from **OPph₃** to **BPph** increased from nearly zero to 54%. Thus, a unique force-responsive RTP effect is achieved based on the enhanced energy transfer under grinding.

To further increase the performance of the phosphorescent material applied, multistage stimulus response effect is considered a good choice. As we all know, the pyridine group shows a stimulus response behavior to proton acid, so the pyridine substituted guest molecules of **Ppy**, **Bppy** and **DBppy** were designed and synthesized (Figure 3a and

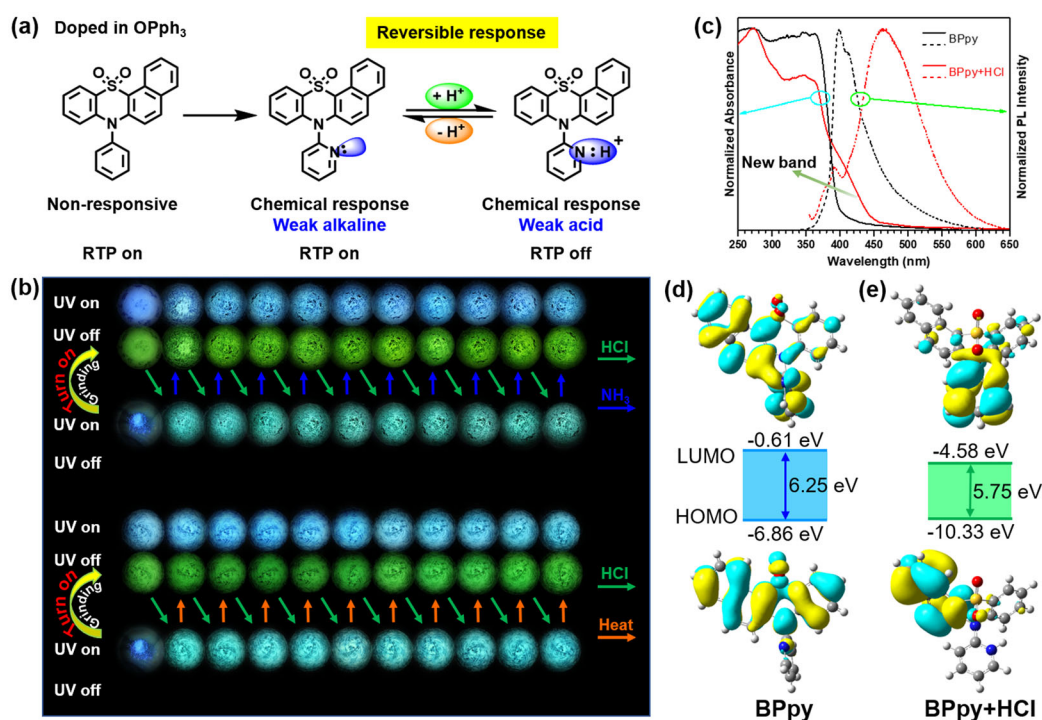


Figure 3. a) **Bppy**'s design concept and stimulus response principle. b) Stimulus-responsive PL behaviors of **Bppy-G** and the corresponding reversible cycle diagram. c) The normalized UV-vis and PL spectra for **Bppy** and **Bppy + HCl**. Calculated HOMO, LUMO orbitals and energy levels, band gaps of d) **Bppy** and e) **Bppy + HCl**.

Scheme S1). **Ppy**, **Bppy** and **DBppy** exhibit similar photochemical properties to their analogues of **Pph**, **BPph** and **DBPph** (Figure S22 to S39). Thus, when they are doped into host of **OPph₃** through co-crystal or grinding, efficient RTP emission could be also observed. Further on, the physically ground powders of **Bppy** and **OPph₃** mixture (1:100 for mass ratio, namely **BPph-G**) are found to show reversible stimulus-responsive RTP effect upon acid-base or acid-heat stimulation. As shown in Figure 3b, the reversible PL changing behavior can be cycled many times for the interaction between nitrogen atom in the pyridine group and proton in acid. Under the irradiation of UV lamp, **BPph-G** emits blue light, then a green afterglow appears after the lamp is turned off. However, when **BPph-G** interacts with protonic acid, namely **BPph-G-HCl**, it would turn to be RTP inactive due to the changed electronic structure of guest, which could be well proved by the newly formed absorption band around 400 nm (Figure 3c). Then, the smaller energy gap leads to the sky-blue fluorescence ($\lambda_{em} = 483$ nm, $\tau = 9.61$ ns, $\Phi_F = 6.31\%$) of **BPph + HCl** (Figure 3d–e, Figure S40, S41 and Table S13).

Since the **Bppy** guest can be dissolved into the **OPph₃** host at molecular level via facile evaporation and grinding methods, the system is of great potential to serve as security ink, stylus/thermal printing paper (Figure 4). First, the stylus/thermal printing paper was prepared based on **Bppy** and **OPph₃**, just as shown in Figure 4a. After stylus printing, the papers look like as a normal one under natural and UV lights (Figure 4b). However, after stopping 254 nm UV excitation, the patterns of “Plum”, “Orchid”, “Bamboo” and “Chrysanthemum” with green afterglow could be observed clearly. In addition, the afterglows of the “dragon” and “phoenix”

patterns printed by thermal printer are brighter (Figure 4c). This is mainly due to thermal stimulation accelerates the movement of molecules and makes the host and guest better contact.

Not only that, environmentally friendly and economical safety inks were prepared based on this doping system, and used for inkjet printing and anti-counterfeiting (Figure S42 and Figure 4d–k). Safety ink based on **Bppy/OPph₃** mixture can be used not only for printing, but also for writing. As shown in Figure 4l, the words “Good luck!” written in three kinds of handwritings can be displayed after the excitation is stopped. After fumigation with acid, the afterglow disappears, and the green afterglow could resume when it is fumigated with NH₃. Thus, the multiple anti-counterfeiting is realized based on the chemical-responsive RTP effect of this doping system. These cases fully illustrate the feasibility of successfully achieving multiple printing and writing methods. The preparation of security ink is closer to commercialization, and it is expected to be used in anti-counterfeiting encryption in the fields of certificates, trademarks, calligraphy and painting.

In summary, a new host–guest doping system with stimulus-responsive RTP characteristics was developed, in which **OPph₃** acted as host and benzo(dibenzo)phenothiazine dioxide derivatives as guest to turn-on RTP by co-crystallization or grinding. Through in detail research, it is found that the energy transfer efficiency from host to guest and the effective ISC ability of the guest are two essential factors for obtaining high phosphorescence efficiency, which maybe provide ideas for the design of organic RTP materials based on host–guest doping. Further on, the introduction of pyridine group into guest achieves reversible fluorescence-phosphor-

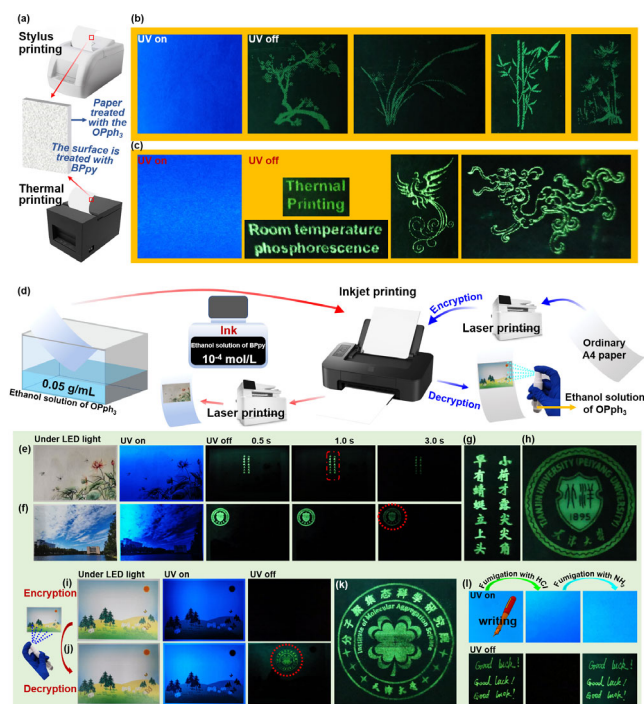


Figure 4. a) Structure for paper materials that can be used for stylus printing and thermal printing. b) Photographs of plum, orchid, bamboo and chrysanthemum patterns printed by stylus printer before and after the UV lamp is turned off. c) Text, phoenix and dragon patterns printed by thermal printer before and after the UV lamp is turned off. d) Using inkjet printing for the production of anti-counterfeiting marks. e), f) Anti-counterfeiting applications. g), h) Partial enlarged view of anti-counterfeiting marks. i), j) Information encryption, in which the ethanol solution of **Bppy** is used as the encryption ink, and the ethanol solution of **OPph₃** is used as the decryption substance. k) Partial enlarged view of Figure (j). (l) Double anti-counterfeiting.

escence switching, then realizing the multistage stimulus-responsive room temperature phosphorescence from grinding to chemical stimulus. In addition, the anti-counterfeiting applications based on the time-resolved characteristic of RTP have been realized by various methods such as stylus printing, thermal printing, inkjet printing, and writing for the first time, which brings RTP materials closer to commercialization. Not only that, the method of obtaining the host–guest phosphorescent system by grinding provides a convenient and effective way to screen for phosphorescent materials.

Acknowledgements

This work was supported by the National Natural Science Foundation of China (no. 21905197) and the starting grants of Tianjin University and Tianjin Government.

Conflict of Interest

The authors declare no conflict of interest.

Keywords: energy transfer · host–guest doping systems · printing · room temperature phosphorescent · stimulus-responsive

- [1] a) S. Xu, R. Chen, C. Zheng, W. Huang, *Adv. Mater.* **2016**, *28*, 9920; b) Kenry, C. Chen, B. Liu, *Nat. Commun.* **2019**, *10*, 2111.
- [2] a) J. Lee, C. Jeong, T. Batagoda, C. Coburn, M. E. Thompson, S. R. Forrest, *Nat. Commun.* **2017**, *8*, 15566; b) R. Kabe, N. Notsuka, K. Yoshida, C. Adachi, *Adv. Mater.* **2016**, *28*, 655.
- [3] a) J. Yang, X. Zhen, B. Wang, X. Gao, Z. Ren, J. Wang, Y. Xie, J. Li, Q. Peng, K. Pu, Z. Li, *Nat. Commun.* **2018**, *9*, 840; b) X. F. Wang, H. Xiao, P. Z. Chen, Q. Z. Yang, B. Chen, C. H. Tung, Y. Z. Chen, L. Z. Wu, *J. Am. Chem. Soc.* **2019**, *141*, 5045; c) Y. Wang, H. Gao, J. Yang, M. Fang, D. Ding, B. Z. Tang, Z. Li, *Adv. Mater.* **2021**, *33*, 2007811.
- [4] a) J. Wei, B. Liang, R. Duan, Z. Cheng, C. Li, T. Zhou, Y. Yi, Y. Wang, *Angew. Chem. Int. Ed.* **2016**, *55*, 15589; *Angew. Chem.* **2016**, *128*, 15818; b) Y. Tian, Y. Gong, Q. Liao, Y. Wang, J. Ren, M. Fang, J. Yang, Z. Li, *Cell Rep. Phys. Sci.* **2020**, *1*, 100052.
- [5] a) Q. Liao, Q. Gao, J. Wang, Y. Gong, Q. Peng, Y. Tian, Y. Fan, H. Guo, D. Ding, Q. Li, Z. Li, *Angew. Chem. Int. Ed.* **2020**, *59*, 9946; *Angew. Chem.* **2020**, *132*, 10032; b) L. Gu, H. Shi, L. Bian, M. Gu, K. Ling, X. Wang, H. Ma, S. Cai, W. Ning, L. Fu, H. Wang, S. Wang, Y. Gao, W. Yao, F. Huo, Y. Tao, Z. An, X. Liu, W. Huang, *Nat. Photonics* **2019**, *13*, 406.
- [6] a) S. Tian, H. Ma, X. Wang, A. Lv, H. Shi, Y. Geng, J. Li, F. Liang, Z. M. Su, Z. An, W. Huang, *Angew. Chem. Int. Ed.* **2019**, *58*, 6645; *Angew. Chem.* **2019**, *131*, 6717; b) W. Zhao, Z. He, J. W. Y. Lam, Q. Peng, H. Ma, Z. Shuai, G. Bai, J. Hao, B. Z. Tang, *Chem* **2016**, *1*, 592; c) H. Zheng, P. Cao, Y. Wang, X. Lu, P. Wu, *Angew. Chem. Int. Ed.* **2021**, *60*, 9500; *Angew. Chem.* **2021**, *133*, 9586.
- [7] Z. Yang, C. Xu, W. Li, Z. Mao, X. Ge, Q. Huang, H. Deng, J. Zhao, F. L. Gu, Y. Zhang, Z. Chi, *Angew. Chem. Int. Ed.* **2020**, *59*, 17451; *Angew. Chem.* **2020**, *132*, 17604.
- [8] a) S. Kuila, S. J. George, *Angew. Chem. Int. Ed.* **2020**, *59*, 9393; *Angew. Chem.* **2020**, *132*, 9479; b) L. Gu, H. Wu, H. Ma, W. Ye, W. Jia, H. Wang, H. Chen, N. Zhang, D. Wang, C. Qian, Z. An, W. Huang, Y. Zhao, *Nat. Commun.* **2020**, *11*, 944.
- [9] a) Q. Li, Z. Li, *Acc. Chem. Res.* **2020**, *53*, 962; b) Y. Tian, X. Yang, Y. Gong, Y. Wang, M. Fang, J. Yang, Z. Tang, Z. Li, *Sci. China Chem.* **2021**, *64*, 445.
- [10] a) R. Kabe, C. Adachi, *Nature* **2017**, *550*, 384; b) S. Hirata, K. Totani, J. Zhang, T. Yamashita, H. Kaji, S. R. Marder, T. Watanabe, C. Adachi, *Adv. Funct. Mater.* **2013**, *23*, 3386; c) T. Zhang, X. Ma, H. Wu, L. Zhu, Y. Zhao, H. Tian, *Angew. Chem. Int. Ed.* **2020**, *59*, 11206; *Angew. Chem.* **2020**, *132*, 11302; d) N. Gan, H. Shi, Z. An, W. Huang, *Adv. Funct. Mater.* **2018**, *28*, 1802657; e) Y. Su, Y. Zhang, Z. Wang, W. Gao, P. Jia, D. Zhang, C. Yang, Y. Li, Y. Zhao, *Angew. Chem. Int. Ed.* **2020**, *59*, 9967; *Angew. Chem.* **2020**, *132*, 10053.
- [11] a) C. Chen, Z. Chi, K. C. Chong, A. S. Batsanov, Z. Yang, Z. Mao, Z. Yang, B. Liu, *Nat. Mater.* **2021**, *20*, 175; b) Y. Wang, J. Yang, M. Fang, Y. Yu, B. Zou, L. Wang, Y. Tian, J. Cheng, B. Z. Tang, Z. Li, *Matter* **2020**, *3*, 449.
- [12] a) J. Yang, M. Fang, Z. Li, *InfoMat* **2020**, *2*, 791; b) M. Louis, H. Thomas, M. Gmelch, A. Haft, F. Fries, S. Reineke, *Adv. Mater.* **2019**, *31*, 1807887; c) Y. Zhou, W. Qin, C. Du, H. Gao, F. Zhu, G. Liang, *Angew. Chem. Int. Ed.* **2019**, *58*, 12102; *Angew. Chem.* **2019**, *131*, 12230; d) J. Ren, Y. Wang, Y. Tian, Z. Liu, X. Xiao, J. Yang, M. Fang, Z. Li, *Angew. Chem. Int. Ed.* **2021**, *60*, 12335; *Angew. Chem.* **2021**, *133*, 12443.

Manuscript received: June 8, 2021

Accepted manuscript online: July 8, 2021

Version of record online: ■■■■■■, ■■■■■■

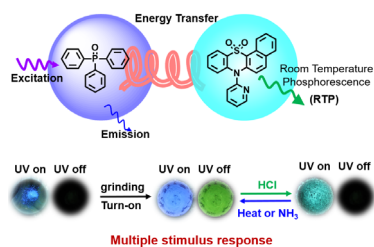
Communications



Luminescence

Y. Tian, J. Yang, Z. Liu, M. Gao, X. Li,
W. Che, M. Fang,* Z. Li* — ■■■■-■■■■

Multistage Stimulus-Responsive Room
Temperature Phosphorescence Based on
Host–Guest Doping Systems



The influence of different conjugation degrees on the quantum yield and lifetime of room temperature phosphorescence in a host–guest system is discussed. Multistage stimulus-responsive RTP characteristics from grinding to chemical stimulus were achieved by introducing a pyridine group into the guest molecule. Anti-counterfeiting printings were realized through various methods, including stylus printing, thermal printing and inkjet printing.